

Side Peaking in Reaction Data Induced by Massive Heavy Ions*

A. J. Baltz

Brookhaven National Laboratory, Upton, New York 11973

(Received 20 October 1976)

The prominent side peak observed in nuclear reaction data induced by massive heavy ions such as Ar, Kr, and Xe is observed to be dominated by quasielastic processes and these processes are interpreted theoretically in terms of the distorted-wave Born approximation (DWBA). Variations of peak location with energy and projectile mass and charge are well reproduced by sample DWBA calculations for particle transfer. Quantal and classical contributions to the angular widths are discussed.

The appearance of total reaction cross sections induced by massive heavy nuclei with single-peaked angular distributions centered approximately at the grazing angle has stirred a great deal of interest recently.¹⁻³ However, in several sets of data where the angular distributions are displayed as a function of the energy loss of the projectilelike fragment, there is a characteristic progression from a narrow single-peaked angular shape for the lowest-energy-loss data, broadening for increasing energy loss, to a relatively flat, forward-peaked angular shape for the most deeply inelastic collisions.^{1,4,5} Thus, there is experimental evidence indicating that the observed side peak in massive-heavy-ion reactions is strongly connected to the lower-energy-loss reactions rather than to deep inelastic processes. At any rate the quasielastic contributions to the sharpness of this peak are crucial and it is the purpose of this Letter to interpret the angular distributions in the quasielastic limit in terms of the distorted-wave Born approximation (DWBA). Several sets of calculations will be presented corresponding to ^{40}Ar on ^{232}Th ,¹ ^{84}Kr on ^{208}Pb ,² and ^{136}Xe on ^{209}Bi .³ The calculations indicate that the side peaking observed with projectiles even as heavy as Xe show qualitative similarity to angular distributions produced, e.g., by the reactions $^{208}\text{Pb}(^{16}\text{O}, ^{15}\text{N})^{209}\text{Bi}$ ⁶ and $^{94}\text{Mo}(^{13}\text{C}, ^{12}\text{C})^{95}\text{Mo}$ ⁷, which are well understood in terms of DWBA. Nevertheless, with the great increase in mass and charge of the projectiles, new features emerge even in quasielastic processes. Our main interest here is in the angular distributions of the final reaction products as a signature of the reaction mechanism, and thus absolute magnitudes of calculated cross sections will be ignored. The DWBA calculations will be for one-proton transfer to specific final states and should be considered as sample or typical angular shapes to be compared with quasielastic data summed over

many final states. Since the projectile velocity is relatively low in all these experiments, the second-order recoil approach⁸ could be used to calculate the DWBA cross sections reliably and relatively quickly, considering the large scattering momenta involved.

We begin by considering a case for which the quasielastic reaction data has been well separated from deep inelastic events, the $Q=0$ bin of the 288- and 379-MeV $^{232}\text{Th}(^{40}\text{Ar}, \text{K})$ data of Artukh *et al.*¹ Cross sections are calculated as $^{232}\text{Th}(^{40}\text{Ar}, ^{41}\text{K})^{231}\text{Ac}$ going to the ground state of both outgoing nuclei. The single-proton bound state was assumed to be $1d_{3/2}$ for ^{41}K and $2d_{3/2}$ for ^{231}Ac , allowing L transfer values of 0, 1, 2, and 3. However, the calculated angular shapes were insensitive to angular momentum transfer and so only $L=0$ computations are shown. The strongly absorptive optical potentials of Birkelund *et al.*⁹ obtained from the elastic scattering $^{238}\text{U}(^{40}\text{Ar}, ^{40}\text{Ar})$ at 286 and 340 MeV were utilized for the distorted waves. The results of the DWBA calculations are shown compared with data in Fig. 1. At both 288 and 379 MeV the angular width is quite well reproduced by the calculations, but it was necessary to change r_0 from 1.131⁹ to 1.25 fm to have the peak angle agree with the data.

Several reasons might be offered for the shift forward of the angular peak of the data from what is predicted from optical parameters. The most obvious is the fact that the DWBA calculations do not include the effect of Coulomb excitation or deformation of the target nucleus. Moreover, the impossibility of separating all quasielastic contributions from the elastic scattering data could affect the r_0 obtained in the optical-model fit. Small Q and L differences of states included in the energy bin of the data have little effect on the calculated position or shape of the peak. For example a 10-MeV change in Q for the 379-MeV

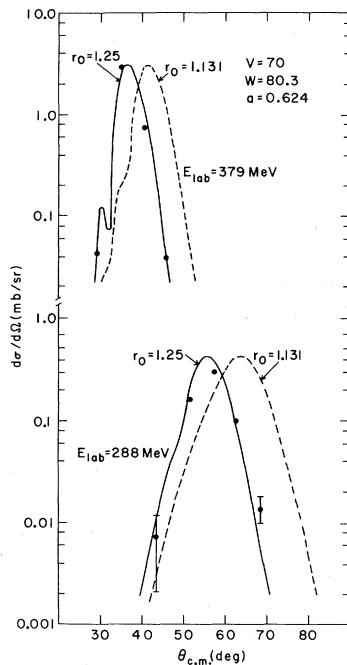


FIG. 1. DWBA calculations of $^{232}\text{Th}(^{40}\text{Ar}, ^{41}\text{K})^{231}\text{Ac}$ (g.s.) $L=0$, one-proton transfer at 288 and 379 MeV compared with data of Ref. 1 for $^{232}\text{Th}(^{40}\text{Ar}, \text{K})$, $Q > -10$ MeV.

calculation corresponds to a change in peak angle of less than a degree.

The qualitative features observed in the quasi-elastic ^{40}Ar -induced reactions are also observed in calculations of typical one-particle transfer contributions to the reaction cross sections for ^{84}Kr on ^{208}Pb ² and ^{136}Xe on ^{209}Bi .³ Figure 2 shows the results of calculations of $^{208}\text{Pb}(^{84}\text{Kr}, ^{83}\text{Br})^{209}\text{Bi}$ compared with the combined quasi-elastic and deep inelastic data of Vandenbosch, Webb, and Thomas at 494, 510, and 718 MeV. The comparison is striking; it suggests that the peak in the reaction angular distribution is well described as a direct quasi-elastic process of the type one is familiar with from data from less-massive heavy-ion projectiles. Of course the comparison is complicated by the fact that there are many channels both quasi-elastic and deep inelastic in the data. However, the fact that such peaks are quasi-elastic connected in the data is indicated by similar 712-MeV data of ^{84}Kr on ^{209}Bi of Huizenga and co-workers⁴ where the peak in the angular distribution is quite pronounced for final states with little energy loss, while the most deeply inelastic events show no peak in the angular distribution. The qualitative difference in shape between the calculation and data seen in

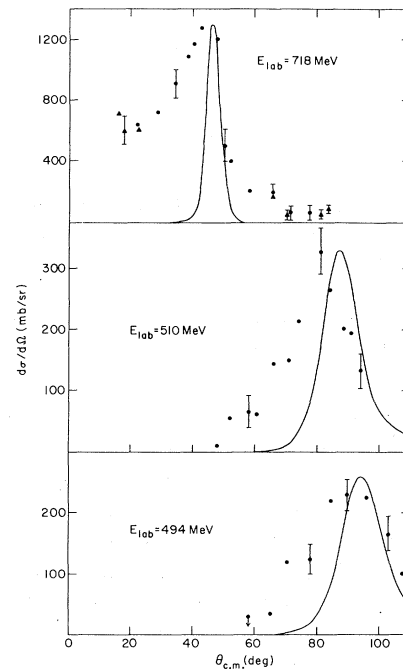


FIG. 2. DWBA calculations of $^{208}\text{Pb}(^{84}\text{Kr}, ^{83}\text{Br})^{209}\text{Bi}$ at 494, 510, and 718 MeV compared with the $^{84}\text{Kr} + ^{208}\text{Pb}$ data of Ref. 2, which data include both quasi-elastic and deep inelastic reaction products. Calculations are for $L=0$ transitions to a $\frac{3}{2}^-$ state in ^{209}Bi . Optical potentials for the 494- and 510-MeV calculations were $V=50$ MeV, $r_V=1.178$ fm, $a_V=1.1$ fm, $W=2.5$ MeV, $r_W=1.282$ fm, and $a_W=0.33$ fm (Ref. 10). For the 718-MeV case, $V=50$ MeV, $r_V=1.129$ fm, $a_V=1.1$ fm, $W=32$ MeV, $r_W=1.211$ fm, and $a_W=0.43$ fm were used (see Ref. 10).

Fig. 2 at 718 MeV may then be understood. While the side peak is dominantly quasi-elastic, the forward rising or orbiting part of the angular shape is due to the more complicated deep inelastic process which we make no attempt to describe here theoretically.

Figure 3 shows a calculation of $^{209}\text{Bi}(^{136}\text{Xe}, ^{137}\text{Cs})^{208}\text{Pb}$ compared with the reaction cross-section data at 1130 MeV. Again the peak of the combined quasi-elastic and deep inelastic reaction data is well described by a typical DWBA calculation for particle transfer. As in the other cases, the calculation using fitted optical potentials peaks at several degrees back of the data, probably for the reasons previously mentioned. Again there is some indication from the similar 1120-MeV Xe on Ta data¹¹ that the side peaking is most pronounced in the quasi-elastic components.

At this point it is interesting to consider possible spreading of the quasi-elastic peak in the angular distribution due to the fact that reactions to

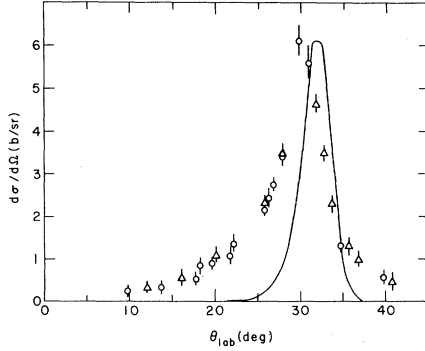


FIG. 3. DWBA calculations of $^{209}\text{Bi}(^{136}\text{Xe}, ^{137}\text{Cs})^{208}\text{Pb}$ at 1130 MeV compared with the combined quasielastic and deep inelastic $^{136}\text{Xe} + ^{209}\text{Bi}$ reaction data of Ref. 3. Calculations are for an $L = 1$ transition to final ground states. Optical parameters are $V = 8.47$ MeV, $W = 6.95$ MeV, $r_0 = 1.30$ fm, and $a = 0.44$ fm (Ref. 3).

many final states are summed (incoherently) in the experimental cross section. What we noted for the Ar reaction, that small changes in Q value have negligible effect on peak angle, turns out to hold *a fortiori* for Kr and Xe projectiles. In these reactions of Coulomb-dominated trajectories, the grazing angle can be approximately related to the interaction radius and the energy of the system through the Coulomb formula for distance of closest approach

$$R = (Z_1 Z_2 e^2 / 2E)(1 + \csc \frac{1}{2}\theta).$$

If one assumes that above the Coulomb barrier, due to strong absorption, the interaction radius for quasielastic processes is approximately independent of energy, then one has an approximate relationship between the energy and scattering angle

$$E/E_{\text{barrier}} \approx \frac{1}{2}(1 + \csc \frac{1}{2}\theta)$$

or, conversely,

$$\theta \approx 2 \csc^{-1}(2E/E_{\text{barrier}} - 1).$$

Notice that the grazing angle depends only on the energy of the system expressed as a ratio of the Coulomb energy. Clearly a small change (≈ 10 MeV) in outgoing-channel energy will have relatively little effect on the position of the peak in the reactions here considered.

In analyzing their $Q = 0$, $^{232}\text{Th}(^{40}\text{Ar}, \text{K})$ data, Artukh *et al.*¹ made use of the simple Strutinsky parametrization¹² of the angular shape to extract the number of partial waves contributing to the transfer cross section. In the 288-MeV case the Δl extracted by this procedure was 12 in contrast

to a Δl of about 30 in the DWBA calculation of Fig. 1. To explain why many more partial waves are contributing to a state of given angular width here we will refer to an extended Strutinsky¹³ model originally put forth to explain deep inelastic reactions.

This model is based on Gaussian shapes, and the angular width of the cross section ξ is composed of two parts and is given by

$$\xi = (\xi_q^2 + \xi_r^2)^{1/2}.$$

$\xi_q = \sqrt{2}/\Delta l$ is the quantum mechanical width of the simple Strutinsky parametrization.¹⁰ This width of angular momenta contributing to a reaction Δl can be roughly related to a width in the radial contribution to the interaction ΔR and a local momentum k , i.e.,

$$\Delta l \approx k\Delta R.$$

Since the radial width ΔR has to do with surfaces and is the same order of magnitude for all reactions, the quantum mechanical width ξ_q varies inversely with scattering momentum, and angular distributions should become quite narrow and sharply peaked with increasing projectile mass. However there is another width,

$$\xi_r = \frac{1}{2}\sqrt{2}(d\theta/dl)\Delta l,$$

which arises from the fact that the classical deflection angle can change appreciably over the l width (Δl) or surface width (ΔR) contributing to the angular distribution. Strutinsky called this effect "dynamic dispersion" and postulated that it might be caused by the nuclear field in deep inelastic collisions.¹³ In the case here studied the effect is mostly due to the Coulomb field and applies to quasielastic transfer.

To continue analysis in this vein, if one assumes a purely Coulomb deflection angle, the dynamic Coulomb dispersion may be written

$$\xi_r \approx \sqrt{2}\eta\Delta l / (l_0^2 + \eta^2),$$

where l_0 is the grazing orbital angular momentum and η the Coulomb parameter. This turns out to be a good approximation to describe the 288-MeV DWBA calculation where the phase derivatives are dominated by the Coulomb field.¹⁴ If one makes use of the Coulomb expression for ξ_r at the peak l of the DWBA calculation then $\xi_r = 6.17^\circ$, which, when combined with the $\xi_q = 2.70^\circ$ implied by the DWBA $\Delta l = 30$, gives $\xi = 6.74^\circ$. Thus the dynamics of the angular width implied by the DWBA calculation is in sharp contrast to the simple parametrization of $\xi = \xi_q = 6.75^\circ$ consistent

with $\Delta l = 12$.

Several general comments can be made concerning the calculations and the data. Most significant is that the side peaking seen in combined quasielastic and deep inelastic reaction data bears a striking resemblance to typical DWBA calculations for a quantum mechanical, one-step process. Of course no attempt has been made here to compute absolute magnitudes of cross sections. Such a calculation would involve a sum of many DWBA calculations weighted by appropriate spectroscopic strengths for the energy, mass, and charge cuts seen in data. Even such a scheme might have to be limited to treatment of one-step processes, while the expectation is that some multistep processes (at least inelastic excitation followed by transfer) should contribute to quasielastic data.

Nevertheless, the use of a simple but realistic quantum mechanical calculation has allowed some realistic analysis of the angular widths. The fact that DWBA calculations fall off rapidly in the forward direction indicates that significant orbiting contributions can be expected only for multistep or deep inelastic processes at these low velocities. The width of the peaks observed is to a large extent determined by the dynamic Coulomb dispersion ξ_r at lower energies (^{40}Ar on ^{232}Th at 288 MeV, ^{84}Kr on ^{208}Pb at 510 MeV, ^{136}Xe on ^{209}Bi at 1130 MeV), while ξ_r decreases to become comparable to the quantum mechanical spreading ($\xi_q = \sqrt{2}/\Delta l$) at higher energies ($^{84}\text{Kr} + ^{208}\text{Pb}$ at 718 MeV). The narrowing of the angular peak with increasing energy comes about as a result of the gradual decrease in importance of the classical spreading due to the dynamic Coulomb dispersion.

I am happy to acknowledge useful discussions with P. D. Bond, R. C. Fuller, and S. Kahana.

*Work supported by the U. S. Energy Research and

Development Administration.

¹A. G. Artukh, G. F. Gridnev, V. L. Mikhaev, V. V. Volkov, and J. Wilczynski, Nucl. Phys. **A215**, 91 (1973).

²R. Vandenbosch, M. P. Webb, and T. D. Thomas, Phys. Rev. Lett. **36**, 459 (1976), and Phys. Rev. C **14**, 143 (1976).

³W. U. Schröder, J. R. Birkelund, J. R. Huizenga, K. L. Wolf, J. P. Unik, and V. E. Viola, Jr., Phys. Rev. Lett. **36**, 514 (1976).

⁴J. R. Huizenga, U. S. Energy Research and Development Administration Progress Report No. COO-3496-56 (unpublished).

⁵P. Russo, R. P. Schmitt, G. J. Wozniak, R. C. Jared, P. Glässel, B. Canvin, J. S. Sventek, and L. G. Moretto, Lawrence Berkeley Laboratory Report No. LBL-5810 (to be published).

⁶D. G. Kovar, B. G. Harvey, F. D. Becchetti, J. Mahoney, D. L. Hendrie, H. Homeyer, W. von Oertzen, and M. A. Nagarajan, Phys. Rev. Lett. **30**, 1075 (1973).

⁷P. D. Bond, C. Chasman, M. J. LeVine, A. Z. Schwarzschild, C. E. Thorn, and A. J. Baltz, Phys. Rev. C **9**, 2001 (1974).

⁸A. J. Baltz, Phys. Rev. C **13**, 668 (1976).

⁹J. R. Birkelund, J. R. Huizenga, H. Freiesleben, K. L. Wolf, J. P. Unik, and V. E. Viola, Jr., Phys. Rev. C **13**, 133 (1976).

¹⁰R. Vandenbosch, M. P. Webb, T. D. Thomas, S. W. Yates, and A. M. Friedman, Phys. Rev. C **13**, 1893 (1976).

¹¹M. S. Zisman, R. Vandenbosch, M. P. Webb, and T. D. Thomas, in ANL Report No. ANL/PHY-76-2, Proceedings of the Symposium on Macroscopic Features of Heavy-Ion Collisions (unpublished), Vol. II, p. 857.

¹²V. M. Strutinsky, Zh. Eksp. Teor. Fiz. **46**, 2087 (1964) [Sov. Phys. JETP **19**, 1401 (1964)].

¹³V. M. Strutinsky, Phys. Lett. **44B**, 245 (1973); H. L. Harney, P. Braun-Munzinger, and C. K. Gelbke, Z. Phys. **269**, 339 (1974); see also Sidney Kahana and A. J. Baltz, "One and Two Nucleon Transfer Reactions with Heavy Ions" (to be published); and D. K. Scott, D. L. Hendrie, L. Kraus, C. F. Maguire, J. Mahoney, M. Terrien, and K. Yagi, Phys. Rev. Lett. **36**, 226 (1976).

¹⁴A. J. Baltz, in ANL Report No. ANL/PHY-76-2, Proceedings of the Symposium on Macroscopic Features of Heavy-Ion Collisions (unpublished), Vol. I, p. 65.